



ORIGINAL ARTICLE

# Separation and enrichment of trace ractopamine in biological samples by uniformly-sized molecularly imprinted polymers

Ya Li<sup>a,b</sup>, Qiang Fu<sup>a,\*</sup>, Meng Liu<sup>a,c</sup>, Yuan-Yuan Jiao<sup>a</sup>, Wei Du<sup>a</sup>, Chong Yu<sup>a</sup>,  
Jing Liu<sup>a</sup>, Chun Chang<sup>a</sup>, Jian Lu<sup>d</sup>

<sup>a</sup>Faculty of Pharmacy, School of Medicine, Xi'an Jiaotong University, Xi'an 710061, PR China

<sup>b</sup>Department of Pharmacy, Northwest Hospital, Xi'an 710004, PR China

<sup>c</sup>Department of Pharmacy, The First Affiliated Hospital of Xinjiang Medical University, Urumqi 830054, PR China

<sup>d</sup>Xian Yang Central Hospital, Xian Yang 71200, PR China

Received 16 May 2012; accepted 20 August 2012

Available online 11 September 2012

## KEYWORDS

Ractopamine;  
Uniformly-sized  
molecularly imprinted  
polymers;  
Solid-phase extraction;  
Multi-step swelling and  
polymerization;  
Separation and  
enrichment

**Abstract** In order to prepare a high capacity packing material for solid-phase extraction with specific recognition ability of trace ractopamine in biological samples, uniformly-sized, molecularly imprinted polymers (MIPs) were prepared by a multi-step swelling and polymerization method using methacrylic acid as a functional monomer, ethylene glycol dimethacrylate as a cross-linker, and toluene as a porogen respectively. Scanning electron microscope and specific surface area were employed to identify the characteristics of MIPs. Ultraviolet spectroscopy, Fourier transform infrared spectroscopy, Scatchard analysis and kinetic study were performed to interpret the specific recognition ability and the binding process of MIPs. The results showed that, compared with other reports, MIPs synthesized in this study showed high adsorption capacity besides specific recognition ability. The adsorption capacity of MIPs was 0.063 mmol/g at 1 mmol/L ractopamine concentration with the distribution coefficient 1.70. The resulting MIPs could be used as solid-phase extraction materials for separation and enrichment of trace ractopamine in biological samples.

© 2012 Xi'an Jiaotong University. Production and hosting by Elsevier B.V.  
Open access under [CC BY-NC-ND license](#).

\*Corresponding author. Tel./fax: +86 29 82655382.

E-mail address: fuqiang@mail.xjtu.edu.cn (Q. Fu).

Peer review under responsibility of Xi'an Jiaotong University.



Production and hosting by Elsevier

## 1. Introduction

Ractopamine (RAC) is a phenethanolamine repartitioning agent belonging to the general class of  $\beta_2$ -receptor agonists, which can significantly increase the lean meat percentage and improve the feed conversion ratio [1,2]. RAC has been widely employed in the livestock industry as a new growth-promoting

feed additive. When the accumulated dose of RAC exceeds a certain value in human beings, it is easy to cause some toxic reactions such as triggering muscle tremor, tachycardia, and muscle pain [3,4]. Although RAC has been approved as a growth promoter in the USA and Australia, it has been officially prohibited to use in the European Union, Japan, and China [5]. However, it is still a frequent phenomenon with illegal use of RAC in meat production as the main reason for acute poisoning [6]. Therefore, accurate and reliable analytical methods for the determination of trace RAC in biological samples are required for the assurance of consumers health.

At present, several analytical methods have been reported for the determination of RAC in biological samples, including immunoassays [7], gas chromatography–mass spectrometry [8], liquid chromatography–mass spectrometry [9,10], enzyme-linked immunosorbent assay [11]. However, these methods not only require tedious pre-treatment procedures but also require expensive instrumentation [12]. Additional time and pretreatment steps are usually required to remove the matrix interference and increase the determination recoveries. The development of a new solid-phase extraction (SPE) adsorbent with high selectivity and specific molecular recognition to detect RAC in biological samples is crucial.

Molecularly imprinted polymers (MIPs), which are cross-linked macromolecules bearing “tailor-made” binding sites for target molecules, have received great attention in recent years [13–15]. The resulting MIPs, not only possess high selectivity and specificity for template molecules, but also exhibit promising physicochemical stability and applicability in harsh chemical media, such as organic solvents, extremes of pH and temperature. The applications of MIPs to chiral separation [16], biomimetic sensors [17], SPE [18], and drug release have been proven useful, and their use as sorbent materials for SPE has become an irresistible trend [19–21]. Although some kinds of MIPs have been prepared for RAC, including surface imprinting materials with a sol–gel method process [22], imprinted polymers coated stir bar [23], and imprinted capillary monolithic stationary phase [24], low adsorption capacity or relatively poor column efficiency towards target molecules are observed. Moreover, it is difficult to control the particle size, shape and porosity, and the tedious grinding and sieving procedures are inevitably needed when bulk polymerization is employed [25]. Hosoya et al. prepared uniformly-sized macroporous polymers by a multi-step swelling and polymerization method, and the obtained polymers possessed uniform particle size, suitable porosity, and good column efficiency towards target molecules [26]. Based on his report, the aim of this paper was to synthesize a high capacity SPE adsorbent with specific recognition ability of trace RAC in biological samples. A convenient, effective and sensitive method to separate and enrich trace RAC in biological samples was established.

## 2. Experimental

### 2.1. Materials and reagents

Methacrylic acid (MAA) was purchased from Tianjin Chemical Reagent Plant (Tianjin, China) and distilled under vacuum to remove inhibitors before use. Trifluoro methacrylic acid (TFMAA) was obtained from Sigma-Aldrich (New Jersey, USA). Ethylene glycol dimethacrylate (EDMA) was obtained

from Aldrich (New Jersey, USA). 2, 2'-Azobisisobutyronitrile (AIBN) was purchased from Shanghai no. 4 Reagent Factory (Shanghai, China) and recrystallized in methanol before use. Salbutamol sulfate (SAL) and clenbuterol hydrochloride (CLB) were obtained from Jinhe Pharmaceutical Co. (Wuhan, China). RAC and terbutaline sulfate (TER) were purchased from Gangzheng Pharmaceutical Co. (Wuhan, China). The structures of these compounds are illustrated in Fig. 1. Acetonitrile was of high performance liquid chromatography (HPLC) grade and all the other reagents were of analytical grade. Water was purified with molelement 1805b (Shanghai, China). Pig liver was obtained from local supermarket. Mice were obtained from Xi'an Jiaotong University Experimental Animal Center (License no: SCSK-shan-2007-001, Xi'an, China).

### 2.2. Preparation of RAC-MIPs

RAC-MIPs were synthesized using MAA as the functional monomer, EDMA as the cross-linker, and toluene as porogen by a multi-step swelling and polymerization method reported previously [27–29]. Briefly, a water dispersion of 1.5 mL of uniformly-sized, polystyrene seed particles was admixed with a microemulsion prepared from 0.48 mL of dibutyl phthalate as an activating solvent, 0.02 g of sodium dodecyl sulfate and 10 mL of water by sonication. The first-step swelling was carried out at 25 °C for 15 h with stirring at 125 rpm until oil microdrops completely disappeared. A dispersion of 0.20 g of AIBN as an initiator, 4 mL of toluene as a porogenic solvent, 10 mL of 4.8% polyvinyl alcohol aqueous solution (PVA) as a dispersion stabilizer, and 12.5 mL of water was added to the dispersion of swollen particles. The second-step swelling was carried out at 25 °C for 2 h with stirring at 125 rpm. A dispersion of 1 mmol of RAC as a template, 4.59 mL of EDMA as a cross-linker, 6 mmol of MAA as a functional monomer, 10 mL of 4.8% PVA and 12.5 mL of water by sonication was added to the dispersion of swollen particles. The third-step swelling was carried out at 25 °C for 2 h with stirring at 125 rpm. After the third-step swelling completed, the polymerization procedure was started at 50 °C under nitrogen atmosphere with stirring at 180 rpm for 24 h. After polymerization, the dispersion of polymerized particles was poured into 250 mL of methanol and the supernatant was discarded after sedimentation of the particles. The polymerized particles were redispersed into methanol, and this procedure was repeated three times in methanol, once in water,

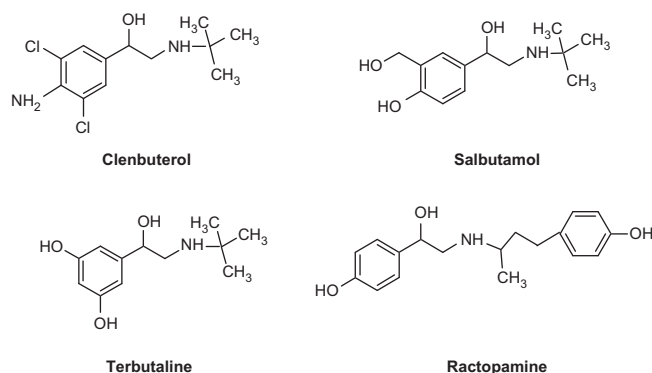


**Figure 1** Structures of RAC and other tested  $\beta_2$ -receptor agonists.

and twice in tetrahydrofuran. The resulting polymerized particles were washed with methanol–acetic acid (80:20, v/v) to remove the template and porogenic agents and dried at 100 °C. Similarly, non-imprinted polymeric microspheres (NIPMs) were prepared by the same procedure except for addition of RAC.

### 2.3. Optimization of RAC-MIPs synthetic conditions

The parameters for preparing polymers were sequentially optimized in this study. 100 mg of RAC-MIPs was mixed with 10 mL of aqueous solution containing RAC. The mixture was shaken (200 times/min) for 3.0 h at 30 °C with an HZ-881 action shaker (Taicang City Scientific Instruments Factory, China) and then filtered through a 0.45 µm filter membrane to remove the adsorbents. The filtrate was measured for the unbound RAC by an SP-2102 UV spectrophotometer 156 (Shanghai Spectrum Instruments Co. Ltd, China) at 226 nm. The same procedure was applied to test the adsorption of NIPMs.

### 2.4. Physical and morphological characterization

The morphological evaluations of RAC-MIPs and NIPMs were performed by scanning electron microscope (SEM) with a JSM-6390A Scanning Microscope (Tokyo, Japan), and the specific surface area was evaluated by an automatic physical chemistry analyzer ASAP-2020C (Mckesson, USA). The infrared absorption spectrum of the polymers between 400 and 4000 cm<sup>-1</sup> was obtained in an FTIR-8400S spectrometer (Shimadzu, Japan).

### 2.5. Binding properties study

In order to investigate the absorption isotherm and kinetic adsorption of RAC-MIPs, 10 mg of RAC was mixed with 10 mL of water solution containing RAC. The mixture was incubated with continuous and horizontal oscillation at 30 °C, and then filtered through a 0.45 µm filter membrane to remove the adsorbents. The unbound RAC in the filtrate was measured by UV spectrometry at 226 nm. The same procedure was applied to test the static adsorption of NIPMs.

### 2.6. The adsorption and selectivity property test

The adsorption and selectivity ability of MIPs and NIPMs were evaluated with RAC, SAL, CLB, and TER. 100 mg of RAC-MIPs and NIPMs were respectively added to a conical flask containing 10 mL of 1 mmol/L water solution of RAC, SAL, CLB, and TER, incubated for 3 h at 30 °C and then filtered through a 0.45 µm filter membrane. The filtrates of RAC, SAL, CLB and TER were determined by UV spectrometry at 226 nm, 276 nm, 245 nm and 276 nm, respectively.

### 2.7. Procedures for the SPE-HPLC determination of RAC using RAC-MIPs

#### 2.7.1. Extraction cartridges

The extraction procedure included packing, conditioning, loading, washing, eluting and regenerating. A methanol dispersion of 2.0 mL of 500 mg of RAC-MIPs dried was packed into an empty 3.0 mL SPE cartridge between two polyethylene cribriform plates. The molecularly imprinted SPE cartridge (MISPE) was firstly rinsed with 6 mL of methanol and 6 mL of water, followed by loading 5.0 mL of a sample solution at a flow rate of 1.0 mL/min in the condition of negative pressure. When the sample loading finished, the cartridge was washed with 10 mL of acetonitrile–water (20:80, v/v) to remove the impurities, and eluted with 10 mL of methanol–acetic acid (90:10, v/v) to desorb RAC. The eluent was then collected and dried with nitrogen at 50 °C. The residue was redissolved with

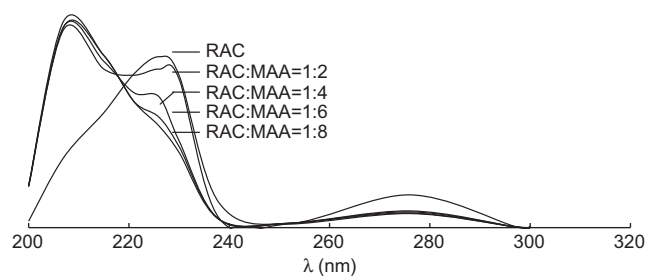


**Figure 2** UV-spectra of RAC under the conditions of the different molar ratios of RAC and MAA.

**Table 1** Optimization of MIPs of synthetic conditions.

Polymer	Monomer		RAC (mmol)	EDMA <sup>a</sup> (v%)	AIBN (mg)	Porogen		$Q_t^b$ (mmol/g)	$k_d$
	MAA (mmol)	TFMAA (mmol)				Toluene (mL)	Chloroform (mL)		
NIPMs	12	0	0	90	0.2	5	0	0.034	0.51
MIPs <sub>1</sub>	4	0	2	90	0.2	5	0	0.044	0.77
MIPs <sub>2</sub>	8	0	2	90	0.2	5	0	0.056	1.29
MIPs <sub>3</sub>	12	0	2	90	0.2	5	0	0.063	1.70
MIPs <sub>4</sub>	16	0	2	90	0.2	5	0	0.057	1.30
MIPs <sub>5</sub>	0	6	2	90	0.2	5	0	0.050	1.00
MIPs <sub>6</sub>	12	0	2	88	0.2	5	0	0.049	0.95
MIPs <sub>7</sub>	12	0	2	92	0.2	5	0	0.030	0.42
MIPs <sub>8</sub>	12	0	2	90	0.2	0	5	0.037	0.55

<sup>a</sup>The volume content of EDMA in the total volume of monomer and EDMA.

<sup>b</sup>Average of three determinations.

1 mL of the mobile phase, filtered through a 0.45  $\mu\text{m}$  filter membrane, and determined by HPLC. HPLC systems consisted of an LC-20A pump, an SPD-20A UV detector (Shimadzu, Japan), and a CS-Light Real Time Analysis Chromatographic Software (Shimadzu, Japan). Turner Kromasil  $\text{C}_{18}$  column (150 mm  $\times$  4.6 mm i.d., 5  $\mu\text{m}$ ) was used with methanol–0.1% ammonium acetate buffer (30:70, v/v) as the mobile phase. The flow rate was 1.0 mL/min and the detective wavelength was 226 nm.

### 2.7.2. Sample preparation

2.0 g of pig liver (determined to be free of RAC) was minced and homogenated with 4 mL saline, and spiked with 200  $\mu\text{L}$  of a series of standard solution of RAC. After incubated for 30 min, the spiked sample was mixed with 6 mL of acetonitrile to remove protein. The resulting extraction was collected and centrifuged, and the supernatant was filtered for the MISPE procedure.

12 healthy mice with the body mass of 20–25 g were fast for 24 h, divided into 2 groups with 6 in each group, and respectively given RAC (40 mg/mL) and normal saline by gavage with 20 mL/(kg  $\cdot$  2 h). After feeding 8 h, their livers were retrieved promptly and then made into liver homogenate. The homogenate about 4 mL was mixed with 6 mL of acetonitrile to remove protein. The resulting extraction was collected and centrifuged, and the supernatants were filtered for the MISPE procedure. The same procedure was applied to the control except for the MISPE procedure.

## 3. Results and discussions

### 3.1. Optimization of MIPs of synthetic conditions

Table 1 illustrates variables viz. the type and the amount of functional monomer, cross-linker and solvents that affected the characteristics of the obtained polymers in terms of capacity, affinity and selectivity for the targeted RAC. To evaluate the adsorption efficiencies of these polymers, the adsorption capacity ( $Q_t$ ) and distribution coefficient ( $k_d$ ) were used. The adsorption capacity was calculated by the following formula [30]:

$$Q_t = (C_0 - C_e)V/W$$

where  $C_0$  is the initial RAC concentration (1 mmol/L),  $C_e$  is the equilibrium concentration of RAC in aqueous solution,  $V$  is the solution volume (10 mL), and  $W$  is the weight of MIPs

or NIPMs (100 mg). The distribution coefficient ( $k_d$ ) is defined as the ratio of the concentrations of RAC at the two phases under the equilibrium state. Two kinds of acidic functional monomers were tested with an expectation of the intermolecular interaction between the template and the monomer. As shown in Table 1, compared with TFMAA, a higher adsorption capacity was achieved by using MAA as the functional monomer under the same amount. With the increase of the amount of MAA from 2 mmol to 6 mmol, both the adsorption capacity ( $Q_t$ ) and distribution coefficient ( $k_d$ ) increased. RAC-MIPs had maximum adsorption capacity when the molar ratio of RAC and MAA reached 1:6. Fig. 2 shows the effect of different molar ratios of RAC and MAA on the UV absorption spectra of RAC. The RAC absorption peak obviously changed with the increase of MAA concentration, which suggested that RAC integrated with MAA with hydrogen bonds [31–33]. Furthermore, cross-linker played a key role in the polymerization process and could fix binding sites firmly in the three-dimensional structure. The obtained RAC-MIPs with 90% of cross-linker showed higher adsorption capacity and greater distribution coefficient. Such was the case with toluene as the solvent compared with chloroform.

Based on the above results, the optimum conditions were established as follows: toluene was selected as the polymerization solvent and MAA as the functional monomer. The molar ratio of RAC and MAA was 1:6. EDMA was 90% (v/v) in the volume of monomer and EDMA. RAC-MIPs<sub>3</sub> was used as the SPE adsorbent in the following experiments.

### 3.2. Physical and morphological characterization

It had been reported that the uniform and rigid microspheres benefits the large embedding of the template molecule and its mass transfer [34]. Fig. 3 presents the SEM images of the MIPs and NIPMs under the magnifications of 20,000. It was evident that both MIPs and NIPMs were almost uniformly distributed with pore diameter and size. Besides, the specific surface area of the resulting MIPs was 91.23  $\text{m}^2/\text{g}$ , and larger than that of NIPMs (79.53  $\text{m}^2/\text{g}$ ), suggesting that MIPs might get a higher adsorption capacity than NIPMs [35].

The infrared spectra of RAC, MIPs before and after depletion of RAC and NIPMs are illustrated in Fig. 4. When RAC was removed from MIPs, the MIPs exhibited similar absorption bands with NIPMs. The broad absorption band at 3428  $\text{cm}^{-1}$  corresponded to the stretching vibration of OH bonds attributed

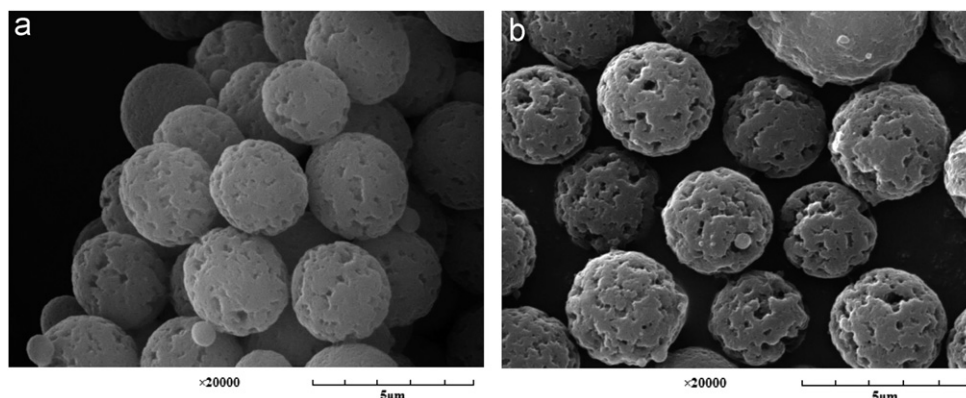
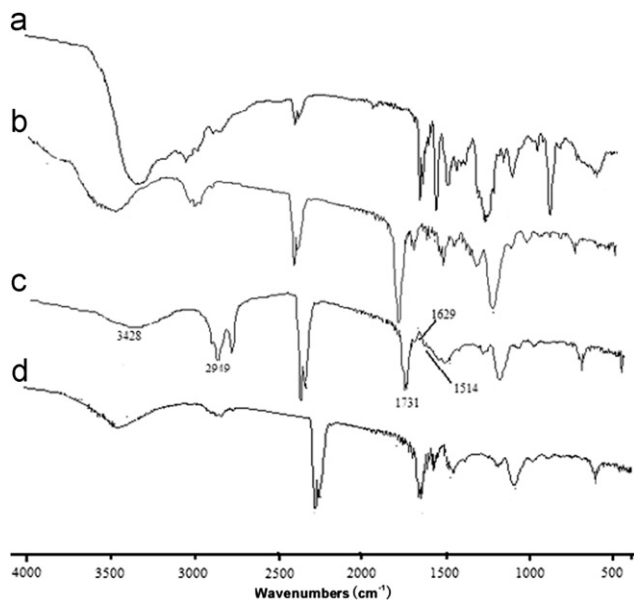
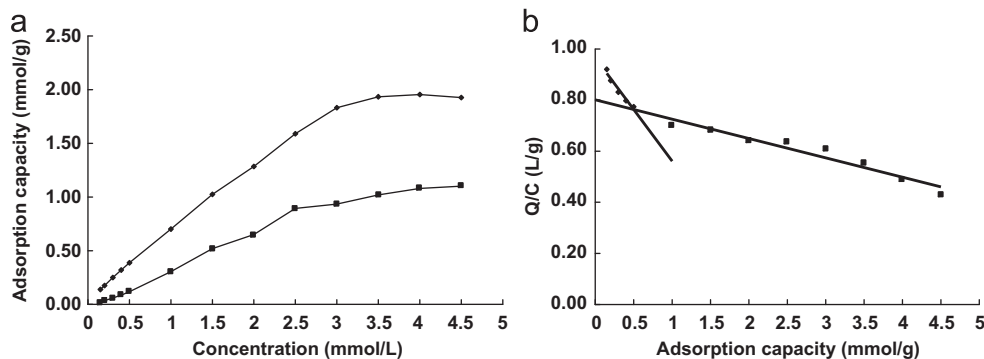


Figure 3 SEM images of RAC-MIPs and NIPMs: the magnifications of 20,000. Key: (a) RAC-MIPs and (b) NIPMs.

to the hydroxyl groups of MAA molecules. The band observed at  $2949\text{ cm}^{-1}$  was indicative of methyl C–H stretching vibration while that at  $1731\text{ cm}^{-1}$  could be attributed to C=O stretching vibration. The absorption peak around  $1629\text{ cm}^{-1}$ , attributed to the stretching vibration of residual vinylic C=C bonds, was discovered on all of the polymers. Curve c in Fig. 4 was the IR spectrum of MIPs before eluting template. The only difference between curve b and curve c was that the broad absorption band corresponded to the stretching vibration of OH bonds was at



**Figure 4** FTIR of the polymers. Key: (a) RAC; (b) RAC-MIPs before the depletion of RAC; (c) RAC-MIPs after the depletion of RAC and (d) NIPMs



**Figure 5** (a) Adsorption isotherm for RAC on RAC-MIPs and NIPMs in aqueous solution. Each value represented the average of three independent measurements and (b) Scatchard analysis of RAC-MIPs for RAC.

**Table 2** Results of Scatchard analysis.

Binging sites	Linear equation	$r^a$	$K_d^b$ (mmol/L)	$Q_{max}^c$ (mmol/g)
Higher affinity sites	$Q/C_e = 0.8010 - 0.0757Q$	0.9550	13.21	10.58
Lower affinity sites	$Q/C_e = 0.9653 - 0.4045Q$	0.9556	2.47	2.38

<sup>a</sup>The correlation coefficient.

<sup>b</sup>The equilibrium dissociation constant.

<sup>c</sup>The maximum adsorption capacity.

$3440\text{ cm}^{-1}$ . The IR absorption changes further indicated that RAC might have reacted with MAA in the imprinted material and form hydrogen binds with MAA.

### 3.3. Adsorption isotherm and Scatchard analysis

The batch rebinding experiments for MIPs or NIPMs were conducted in water to ensure relatively high concentration of RAC and prevent the polymers swelling. Fig. 5(a) shows that the adsorption capacity ( $Q_t$ ) of both MIPs and NIPMs increased gradually with the RAC concentration increasing, but their obvious distinction was that the adsorption capacity ( $Q_t$ ) of MIPs was much more than that of NIPMs. It was especially notable that the difference of the adsorption capacity ( $Q_t$ ) became enlarged with the increase of the RAC concentration within the observed range. The binding isotherms could be estimated by application of the Scatchard analysis model [36,37], i.e.  $Q/C_e = (Q_{max} - Q)/K_d$ , where  $Q_{max}$  is the maximum adsorption capacity,  $K_d$  is the equilibrium dissociation constant, and  $C_e$  represents the equilibrium concentration of RAC in solution, respectively. Fig. 5(b) shows that the Scatchard plot of MIPs revealed two straight lines with different slopes, indicating that the binding sites in MIPs could be classified into two distinct groups corresponding to the high- and low-affinity binding sites. The results of Scatchard analysis are listed in Table 2. From Scatchard equation, the maximum adsorption capacity ( $Q_{max1}$ ) and the equilibrium dissociation constant ( $K_{d1}$ ) of the higher affinity binding sites were calculated to be  $Q_{max1} = 10.58\text{ mmol/g}$  and  $K_{d1} = 13.21\text{ mmol/L}$ . In the same way,  $Q_{max2}$  and  $K_{d2}$  of the lower affinity bonding sites were  $Q_{max2} = 2.38\text{ mmol/g}$  and  $K_{d2} = 2.47\text{ mmol/L}$ .

### 3.4. Uptake kinetics of RAC by MIPs and NIPMs

The uptake kinetics of RAC by MIPs and NIPMs was examined at 1 mmol/L RAC concentration and the results are illustrated in Fig. 6. It was obvious that both MIPs and NIPMs had fast uptake kinetics, and the binding equilibrium was almost obtained within 60 min. The saturating time of NIPMs was shorter than that of MIPs, owing to the surface non-specific bonding sites [38].

### 3.5. The adsorption and selectivity property of MIPs and NIPMs

Table 3 shows the adsorption capacity of MIPs towards RAC and some other  $\beta_2$ -receptor agonists, in which the imprinting factor ( $\beta$ ) and selectivity coefficient ( $\alpha$ ) were introduced. Herein, the imprinting factor ( $\beta$ ) is defined as the ratio of the adsorption capacity of MIPs ( $Q_m$ , mmol/g) to the adsorption capacity of NIPMs ( $Q_n$ , mmol/g). The selectivity coefficient ( $\alpha$ ) is defined as the ratio of distribution coefficient between two different compounds, i.e.  $\alpha = k_{d1}/k_{d2}$ .

The results showed that the adsorption capacity of MIPs (0.063 mmol/g) was 1.85-fold that of NIPMs (0.034 mmol/g) at 1 mmol/L RAC concentration. The selectivity coefficient ( $\alpha$ ) of SAL, TER, and CLB was 2.26, 11.40, and 29.83 for MIPs and 1.32, 3.16, and 12.26 for NIPMs respectively. Compared with other reports [39], the resulting RAC-MIPs had a higher adsorption capacity and a better specific recognition ability, which could be ascribed to the characteristics of uniformly distributed polymeric microspheres of RAC-MIPs.

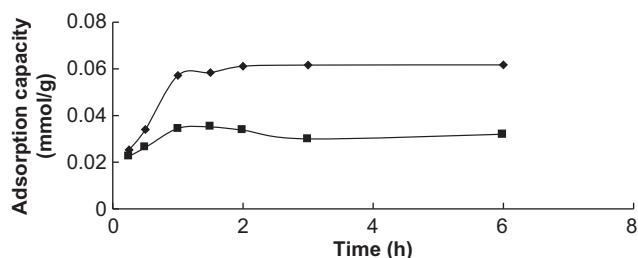


**Figure 6** The adsorption time plot of RAC on RAC-MIPs and NIPMs.

### 3.6. Application of MIPs-SPE for the pretreatment and enrichment of RAC in biological samples

MIPs were used as specifically selective SPE materials coupled with HPLC for the determination of RAC in biological samples. The eluent was critical for the extraction of RAC. Therefore, the type and construction of elution solution were investigated and the results showed that methanol-acetic acid (90:10, v/v) was the best choice for eluting RAC.

To validate the applicability of the proposed method, the linearity and the limit of detection (LOD) were investigated. A linearity was obtained in the range of 0.2–25.0 mg/L for RAC, and the equation was  $Y = 72574X + 36423$  with a correlation coefficient ( $r$ ) 0.9974. The LOD (calculated from signal/noise=3:1) was 0.02 mg/L. The established MIPs-SPE-HPLC method was applied to the spiked pig liver set with three levels of RAC (0.5, 2.0 and 10.0 mg/L). At each

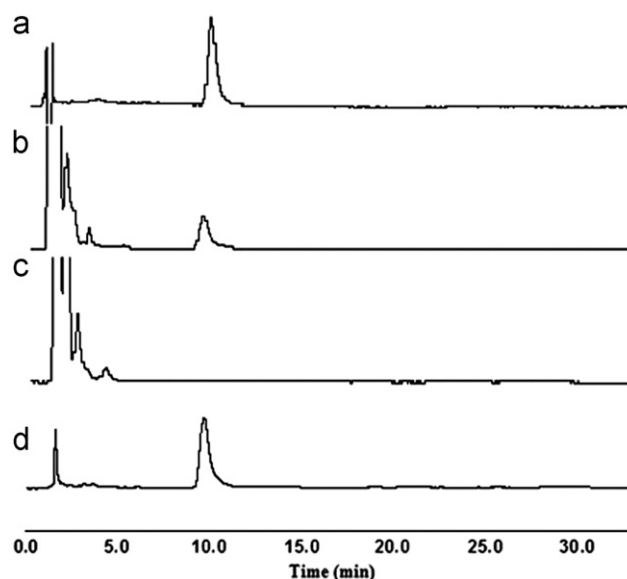


**Figure 7** The chromatograms of the mice liver samples with RAC. Key: (a) standard solution of RAC; (b) mice liver sample without MIPs pretreatment; (c) blank liver; (d) mice liver sample with MIPs pretreatment. HPLC conditions: column, Turner Kromasil C<sub>18</sub> column (150 mm × 4.6 mm i.d., 5 μm); mobile phase, methanol–0.1% ammonium acetate buffer (30:70, v/v); flow rate, 1.0 mL/min; detection wavelength, 226 nm; loaded volume, 20 μL.

**Table 3** The imprinting factor ( $\beta$ ) and selectivity coefficient ( $\alpha$ ) of MIPs and NIPMs for RAC in aqueous solution.

Compound	$Q_i$ (mmol/g)		$\beta^a$	$\alpha^b$	
	MIPs	NIPMs		MIPs	NIPMs
RAC	0.063	0.034	1.85		
SAL	0.043	0.028	1.54	2.26	1.32
CLB	0.013	0.014	0.93	11.40	3.16
TER	0.005	0.004	1.35	29.83	12.26

<sup>a</sup>The imprinting factor,  $\beta = Q_m/Q_n$ .

<sup>b</sup>Selectivity coefficient,  $\alpha = k_{d1}/k_{d2}$ .

**Table 4** The relative recoveries of RAC ( $n=5$ ).

Spiked liver samples (mg/L)	Average concentrations found (mg/L)	Recovery (%)	RSD (%)
10.0	10.26	102.6	2.4
2.0	1.97	98.5	2.8
0.5	0.49	98.0	5.7

concentration, five measurements were performed. The results are shown in Table 4, and the recoveries of the pig liver samples spiked with 0.5, 2.0 and 10.0 mg/L of RAC were 98.0%, 98.5% and 102.6%, respectively, with RSD ranging from 2.4% to 5.7%.

The established MIPs-SPE-HPLC method was also used to mice real samples. Typical chromatograms are shown in Fig. 7. The peaks of interferent components decreased dramatically and the RAC peak increased after the SPE procedures, which suggested that RAC of the mice samples has been purified and enriched efficiently.

#### 4. Conclusions

We prepared uniformly-sized MIPs for RAC by a multi-step swelling and polymerization method using MAA as a functional monomer, and EDMA as a cross-linker and toluene as a porogen. MIPs had high affinity, selectivity and adsorption capacity for RAC, and could be used as sorbents for SPE. The established MIPs-SPE-HPLC method could be used for the determination of trace RAC in biological samples.

#### Acknowledgments

This work was financially supported by the National Natural Science Foundations of China (no. 30873193 and no. 81173024) to professor Q. Fu. The authors also express their gratitude to professor Jun Haginaka from Mukogawa Women's University for his great help in the polymer preparation.

#### References

- [1] K.A. Ross, A.D. Beaulieu, J. Merrill, et al., The impact of ractopamine hydrochloride on growth and metabolism, with special consideration of its role on nitrogen balance and water utilization in pork production, *J. Anim. Sci.* 89 (2011) 2243–2256.
- [2] N.O. Amaral, E.T. Fialho, V.S. Cantarelli, Ractopamine hydrochloride in formulated rations for barrows or gilts from 94 to 130 kg, *Rev. Bras. Zootec.* 38 (2009) 1494–1501.
- [3] T.A. Peterla, C.G. Scanes, Effect of beta-adrenergic agonists on lipolysis and lipogenesis by porcine adipose tissue in vitro, *J. Anim. Sci.* 68 (1990) 1024–1029.
- [4] J.F. Martinez-Navarro, Food poisoning related to consumption of illicit beta-agonist in liver, *Lancet* 336 (1990) 1311.
- [5] FDA (Food and Drug Administration). New animal drugs for use in animal feeds: Ractopamine hydrochloride, USA:FDA 69 (2004) 88.
- [6] S. Muirhead, CVM approves leanness enhancer for use in food production animals, *Feed Stuffs* 72 (2000) 11.
- [7] X.H. Qi, W.L. Shelver, Y.Y. Dong, et al., Microfluidic immunochemical ractopamine analysis, *Abstr. Pap. Am. Chem. Soc.* 232 (2006) 600.

- [8] J.P. Wang, X.W. Li, W. Zhang, et al., Development of immunoaffinity sample-purification for GC–MS analysis of ractopamine in swine tissue, *Chromatographia* 64 (2006) 613–617.
- [9] J. Pleadin, A. Vulic, N. Persi, et al., Correlation of ELISA and LC-MS/MS methods in determination of urinary ractopamine residual concentrations in treated pigs, *Toxicol. Lett.* 205 (2011) 145–145.
- [10] S. Eshaq, C.C. Sin, J. Sami, et al., Determination of ractopamine in animal tissues by liquid chromatography-fluorescence and liquid chromatography/tandem mass spectrometry, *Anal. Chim. Acta* 483 (2003) 137–145.
- [11] D.G. Pei, X. Wang, M.L. Xu, et al., Development of an ELISA for ractopamine, *Chin. J. Health Lab. Tech.* 20 (2010) 319–320.
- [12] C.H. Qu, X.L. Li, L.X. Zhang, et al., Simultaneous determination of cimaterol, salbutamol, terbutaline and ractopamine in feed by SPE coupled to UPLC, *Chromatographia* 73 (2011) 243–249.
- [13] Y. Lei, M. Klaus, The technique of molecular imprinting-principle, state of the art, and future aspects, *J. Inclusion Phenom. Macrocyclic. Chem.* 41 (2001) 107–113.
- [14] L.X. Chen, S.F. Xu, J.H. Li, Recent advances in molecular imprinting technology: current status, challenges and highlighted applications, *Chem. Soc. Rev.* 40 (2011) 2922–2942.
- [15] B.J. Si, C.B. Chen, J. Zhou, New-generation of molecular imprinting technique, *Prog. Chem.* 21 (2009) 1813–1819.
- [16] A. Elijan, Q. Fu, Q. Fang, et al., In situ polymerization preparation of chiral molecular imprinting polymers monolithic column for amlodipine and its recognition properties study, *J. Polym. Res.* 17 (2010) 401–409.
- [17] Y.X. Chen, B.J. Gao, G.M. Jiang, et al., Constituting chiral caves by using novel surface-molecular imprinting technique and realizing chiral separation of enantiomers of amino acid, *Acta Chim. Sinica.* 69 (2011) 1705–1714.
- [18] F. Barahona, E. Turiel, E.A. Martin, Molecularly imprinted polymer grafted to porous polyethylene frits: a new selective solid-phase extraction format, *J. Chromatogr. A* 40 (2011) 7065–7070.
- [19] J. Mehran, M.A. Abdol, H.N. Mohammad, et al., Solid-phase extraction of tramadol from plasma and urine samples using a novel water-compatible molecularly imprinted polymer, *J. Chromatogr. B* 878 (2010) 1700–1706.
- [20] R.N. Rao, P.K. Maurya, S. Khalid, Development of a molecularly imprinted polymer for selective extraction followed by liquid chromatographic determination of sitagliptin in rat plasma and urine, *Talanta* 85 (2011) 950–957.
- [21] W. Christine, L. Fredrik, F. Maurizio, et al., Evaluation of MISPE for the multi-residue extraction of  $\beta$ -agonists from calves urine, *J. Chromatogr. B* 804 (2004) 85–91.
- [22] S. Wang, L. Liu, G.Z. Fang, et al., Molecularly imprinted polymer for the determination of trace ractopamine in pork using SPE followed by HPLC with fluorescence detection, *J. Sep. Sci.* 32 (2009) 1333–1339.
- [23] Z.G. Xu, Y.F. Hu, Y.L. Hu, et al., Investigation of ractopamine molecularly imprinted stir bar sorptive extraction and its application for trace analysis of  $\beta_2$ -agonists in complex samples, *J. Chromatogr. A* 1217 (2010) 3612–3618.
- [24] J.X. He, G.Z. Fang, Q.L. Deng, et al., Characterization and application of organic-inorganic hybrid ractopamine multi-template molecularly imprinted capillary monolithic column, *Anal. Chim. Acta* 692 (2011) 57–62.
- [25] Y.L. Hu, R.J. Liu, Y.W. Li, Investigation of ractopamine-imprinted polymer for dispersive solid-phase extraction of trace  $\beta$ -agonists in pig tissues, *J. Sep. Sci.* 33 (2010) 2017–2025.
- [26] K. Hosoya, K. Yoshizako, N. Tanaka, et al., Uniform-size macroporous polymer-based stationary phase for HPLC prepared through molecular imprinting technique, *Chem. Lett.* 23 (1994) 1437–1438.
- [27] Q. Fu, H. Sanbe, C. Kagawa, et al., Uniformly sized molecularly imprinted polymer for (S)-nilvadipine comparison of chiral recognition ability with HPLC chiral stationary phases based on a protein, *Anal. Chem.* 75 (2003) 191–198.

- [28] Y.C. Li, Q. Fu, Q.Q. Zhang, et al., Preparation and evaluation of uniform-size (-)-ephedrine-imprinted polymeric microspheres by multi-step swelling and suspension polymerization, *Anal. Sci.* 22 (2006) 1355–1360.
- [29] H. Sambe, K. Hoshina, J. Haginaka, Molecularly imprinted polymers for triazine herbicides prepared by multi-step swelling and polymerization method. Their application to the determination of methylthiotriazine herbicides in river water, *J. Chromatogr. A* 1152 (2007) 130–137.
- [30] X.M. Zheng, W.P. Tu, Preparation of monodisperse molecularly imprinted polymer beads by a single-step swelling and polymerization method, *J. Chem. Eng. Chin. Univ.* 21 (2007) 116–121.
- [31] D.M. Chi, L.Q. Su, X.S. Deng, et al., Development in the research of the selection methods of functional monomer in molecular imprinting, *Chem. Ind. Times* 23 (2009) 55–57.
- [32] Y. Lu, C.X. Li, H.H. Zhang, et al., Study on the mechanism of chiral recognition with molecularly imprinted polymers, *Anal. Chim. Acta* 489 (2003) 33–43.
- [33] J. Mahony, A. Molinelli, K. Nolan, et al., Anatomy of a successful imprint: analysing the recognition mechanisms of a molecularly imprinted polymer for quercetin, *Biosens. Bioelectron.* 21 (2006) 1383–1392.
- [34] K. Alexander, E.D. Mark, Investigations into the mechanisms of molecular recognition with imprinted polymers, *Macromolecules* 32 (1999) 4113–4121.
- [35] X.M. Zheng, R.Y. Fan, W.P. Tu, The relationships between structure and properties of molecularly imprinted polymeric microspheres, *J. Chem. Eng. Chin. Univ.* 24 (2010) 492–497.
- [36] Z.K. George, N.B. Dimitrios, K.L. Nikolaos, Selective separation of basic and reactive dyes by molecularly imprinted polymers (MIPs), *Chem. Eng. J.* 149 (2009) 263–272.
- [37] Y.F. Luo, P. Huang, Q. Fu, et al., Preparation of monolithic imprinted stationary phase for clenbuterol by in situ polymerization and application in biological samples pre-treatment, *Chromatographia* 74 (2011) 693–701.
- [38] X.M. Zheng, W.P. Tu, Influential factors of capabilities of combination and recognition in molecularly imprinted polymers, *Mater. Rev.* 18 (2004) 57–59.
- [39] Y.W. Tang, G.Z. Fang, S. Wang, et al., Covalent imprinted polymer for selective and rapid enrichment of ractopamine by a non-covalent approach, *Anal. Bioanal. Chem.* 401 (2011) 2275–2282.